

SEISMIC PERFORMANCE OF A NOVEL GUYED SYSTEM FOR THE SUPPORT OF OFFSHORE WIND-TURBINES

Fani GELAGOTI¹, Maria ANTONIOU, Ioannis ANASTASOPOULOS

ABSTRACT

The paper is exploring the potential of a cost-efficient and easy-to-install scheme for the support of large capacity offshore wind turbines (OWTs) in intermediate water depths. In the proposed scheme the lateral stability of the wind-turbine tower is provided by a taut mooring system comprising of four pre-stressed tendons anchored to the seabed by means of suction caissons. To assist the installation process, a single pier-pin connection is implemented at the tower base sitting on top of a circular surface footing. The efficacy of the proposed solution is demonstrated numerically by investigating the performance of the NOWITECH 10^{MW} reference turbine installed in water depth of 50m in the earthquake prone Adriatic basin.

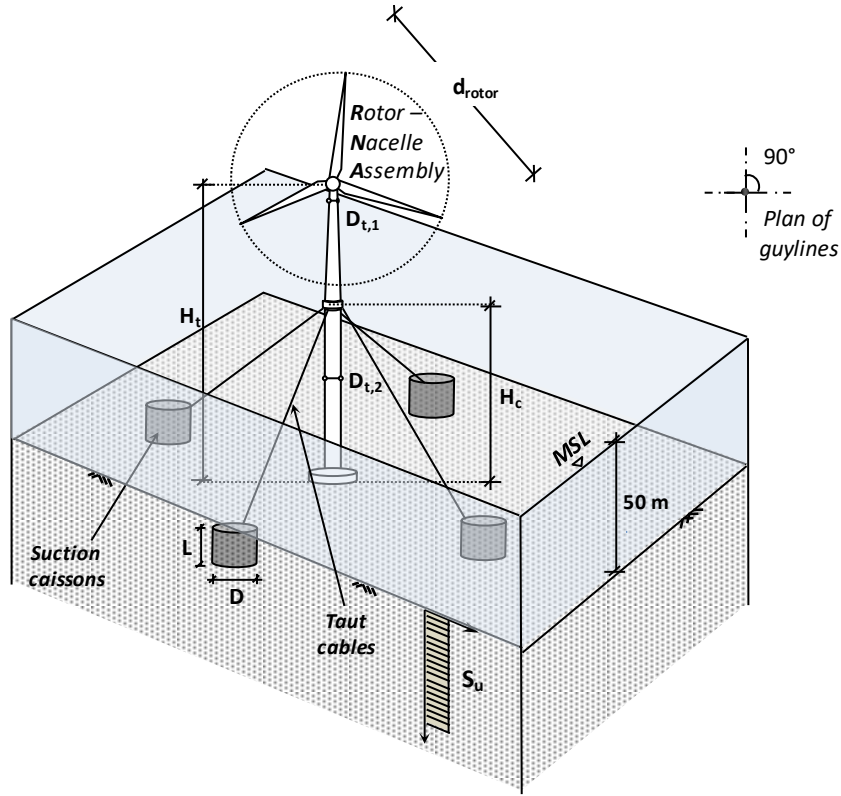
It is concluded that the proposed guyed OWT is a rather resilient earthquake scheme that undertakes the seismically-induced deformations, through controlled displacements at the cable connection point, protecting the tower from excessive structural stressing and undesirable inelastic deformations. Controlling factor of the performance of the OWT is the mobilized pull-out resistance of the suction anchors during earthquake shaking. Under perfectly ‘sealed’ conditions, passive suction is being developed beneath the lid contributing to the overall excellent seismic performance of the OWT. On the other hand, if the development of suction cannot be relied upon (e.g. case of improper installation), caissons may display non-trivial permanent deformations, which depending on the level of seismic shaking, may even result to loss of cable tension.

Keywords: Offshore Wind-turbine; soil-structure-interaction; earthquake; suction anchors; taut moorings.

1. INTRODUCTION

As the world’s energy demands rapidly rise, offshore wind farms increase in size and migrate into deeper waters, where the wind blows more strongly and steadily. The need arises, to replace traditional fixed – based foundations with new, cost – efficient and easy-to-install concepts (World Energy Council, 2016). Novel ideas, such as floating or semi floating concepts are being currently under continuous development by the offshore industry, but despite the promise, floating wind technology is still nascent (Bulder et al, 2002; Bastick, 2009; Bratland, 2009; Weinstein, 2009). Motivated by this reality, the objective of this paper is to explore the potential of a transitional supporting scheme for offshore wind-towers that may be best exploited for intermediate water depths. The proposed system comprises a relatively compliant tower that goes all the way down to the seabed. Yet, instead of a massive foundation, the lateral stability of the tower is provided by a taut mooring system comprising of four pre-stressed tendons anchored to the seabed by means of suction caissons (Fig. 1). The system’s performance is examined under the concurrent action of environmental and earthquake loading, while two distinct assumptions for the suction caissons are taken into account: (a) passive suction developed under the caisson lid is relied upon and (b) passive suction is completely ignored.

¹ Corresponding Author, Postdoctoral Researcher, National Technical University of Athens



	$D_{t,1}$: m	t_1 : m	$D_{t,2}$: m	t_2 : m	H_t : m	d_{rotor} : m	Nacelle & Rotor Mass : t_n
10^{MW}	3.6	0.021	6	0.05	150	140.4	400

Figure 1. The 10MW offshore wind turbine under consideration, founded on the proposed guyed support structure in a homogeneous clay stratum, along with its key geometrical properties.

2. CASE STUDY: APPLICATION OF THE PROPOSED CONCEPT TO A 10MW OWT IN THE ADRIATIC SEA

2.1 Numerical modelling

The NOWITECH 10MW reference turbine is assumed to be installed in a water depth of 50m in the seismically active region of North-Western Adriatic Sea. The dimensions of the reference turbine are summarized in Fig. 1. The seabed at the installation location consists of a homogeneous clay stratum with undrained shear strength $S_u = 100$ kPa (Tonni et al, 2016). The turbine tower is being braced with four pretensioned cables, equally spaced around at 90° intervals and anchored to the seabed by means of suction caissons (Fig. 1). Each mooring line comprises 4 galvanized steel spiral strands (each of area $A_s = 11677$ mm², modulus of elasticity $E_s = 170$ GPa and ultimate breaking strength $F_{ult} = 17.5$ MN) pretensioned at $T_o = 6$ MN, providing an initial pretension over breaking strength ratio (T_o/F_{ult}) equal to 8.6%, which complies with the 8 - 15% interval proposed by TIA-222-F (1996) standards. In the proposed scheme, a single mooring connection - just beneath the rotor blades and few meters above the MSL (mean sea level) - is assumed. Lateral deformations of the compliant tower are structurally controlled by properly adjusting the design tension of the prestressed tendons. Pretensioned guy lines provide the necessary restoring forces to the imposed environmental loading, while the turbine tower is simply supported at its base by means of a circular surface footing. The tower is connected to the surface footing with a sole universal joint, as in most cases of such compliant guyed support schemes. As such, the surface footing is not subjected to moment loading, while the bending at the lower tower sections is significantly reduced, allowing for material savings.

The performance of the proposed system is analyzed numerically implementing a 3D finite element (FE) model in ABAQUS software (Dassault Systèmes, 2013). For the sake of simplicity, all environmental loads are assumed to be acting collinearly on the exact same plane throughout this study, thus the out of plane cable lines are conservatively considered not to contribute to the system’s lateral resistance. A typical view of the entire system F.E. model geometry is illustrated in Fig. 2. The OWT tower is modelled with 3-D elastic beam elements (B31) of variable diameter D_t and thickness t_t to correctly account for the tapered shape of the tower-section. The rotor- nacelle assembly is modelled as a concentrated mass at the top of the tower, while elastic 3D truss elements (T3D2) of zero bending and torsional stiffness are employed for the modelling of pretensioned cables. Hydrodynamic masses associated with the submerged parts of the cables and the turbine tower are calculated according to the formulas of Chen and Chung (1976) for a single cylinder in an infinite fluid and are incorporated into the finite element model as concentrated masses, distributed along the length of the submerged structural parts.

The mesh boundaries are placed appropriately to ensure no interference of boundary-effects on the foundation response. Displacement boundary conditions prevent the out-of-plane movement of the vertical face as well as the horizontal displacement at the lateral nodes, while the model base is fixed in all three directions. A pinned connection is implemented between the cables and the top plate of the caissons. Soil is represented by eight-node hexahedral continuum elements (C3D8) and is simulated herein as one-phase medium of undrained shear strength S_u . Its non-linear stress-stain behavior is described by a simplified kinematic hardening model that follows a Von Mises failure criterion with an associated flow rule (Anastasopoulos et al., 2011). For the full description of the nonlinear behavior of a clay specimen, only three terms need to be determined: the strength S_u , the ratio of G/S_u (where G the initial kinematic hardening modulus) and the parameter γ .

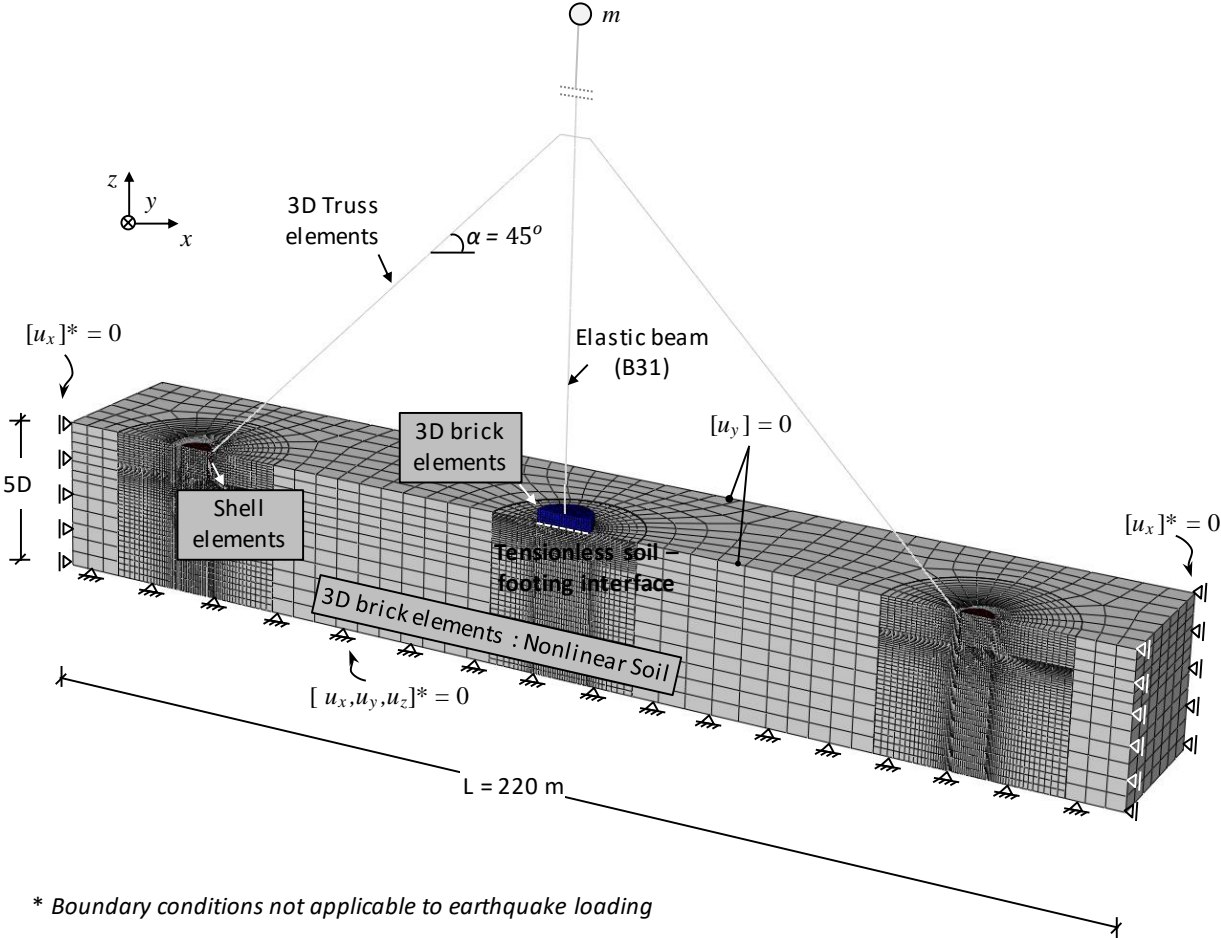


Figure 2. Finite element mesh of the soil-foundation-structure system.

Linear elastic shell elements are used for the simulation of the suction caissons, assuming caissons of diameter (D) and skirt length (L). To numerically model ‘sealed’ or ‘unsealed’ conditions, special-purpose contact elements of zero thickness (available in the ABAQUS library) are introduced between the soil and the caisson.

- For perfectly “sealed” conditions, fully bonded conditions are assumed between the soil and caisson parts, transposing the failure mechanism to the base of the caisson.
- For “unsealed” conditions, tensionless interfaces are used between the soil and caisson parts (skirts & lid), allowing for vertical sliding and detachment.

For both interface scenarios, the shearing resistance is assumed to reach a limiting value equal to a fraction of the undrained shear strength αS_u , to account for possible soil remoulding during installation. Following the API RP 2A-WSD (2000) recommendations for stiff clays, an adhesion factor $\alpha=0.5$ has been adopted.

2.2 ULS and SLS Design

Design is performed considering Consequence Class 2, as defined by API RP 2A-WSD (2000) and DNV-OS-E301 (2010). Environmental loading calculations are based on the results of a site-specific meteocean study of the Adriatic Sea, reported by the EU Funded Research Program JABACO. For the Ultimate Limit State (ULS) and Serviceability Limit State design (SLS) purposes, environmental loads are simulated as steady constant forces – a reasonable assumption given the extremely low frequency nature of wind / wave loads compared to the eigenfrequency of the turbine. For ULS conditions, a maximum significant wave height of $H_{s,100} = 12.1$ m and fundamental period $T_p = 14.4$ sec is adopted, combined with an ocean current of constant speed $U_c = 1.3$ m/s. Using the Morison’s equation (Morison, 1950), this extreme sea state is translated into hydrodynamic loading of $F_{\text{wave,ULS}} = 4.5$ MN, acting at approximately $h_w = 42$ m above the mudline. Moreover, the turbine is subjected to a maximum wind speed of 25 m/s (corresponding to the cut-out speed of the turbine), inducing a concentrated wind thrust of $F_{\text{wind,ULS}} = 2.4$ MN on the rotor. For SLS conditions, the adopted normal wave loads correspond to a significant wave height of $H_{s,l} = 2.6$ m and $T_p = 9.12$ sec, which produce a hydrodynamic loading of $F_{\text{wave,SLS}} = 1.0$ MN on the tower, while a wind speed of 13.1 m/s is considered, resulting in a concentrated wind thrust of $F_{\text{wind,SLS}} = 1.1$ MN.

The circular footing is designed to sustain vertical loading (stemming from the structure’s dead weights and the vertical component of initial pretension T_o) in combination with horizontal loading, introduced by the external environmental actions. For the specific numerical example, a footing of diameter $D_f = 11$ m and height $h_f = 2.5$ m was introduced which yields safety factors of $SF_v = 2.5$ and $SF_h = 2.1$ against vertical and horizontal loads respectively.

The anchoring system should be adequately designed to safely sustain the pull-out tension loading from the taut moorings without displacing excessively. Yet, the maximum available mobilized capacity of the suction anchors critically depends on the degree of suction that can be relied upon (Randolph & House, 2002). Under perfectly ‘sealed’ conditions (i.e., when suction is developed beneath the caisson lid), a ‘reverse end bearing’ mechanism takes place, where the inner soil plug is uplifted, and the outer soil is dragged beneath the bucket, generating augmented resistance values. If the ‘sealing’ is inefficient, (i.e., in case of improper installation or when the soil permeability is very high to sustain suction) failure will occur in the form of sliding along the wall of the caisson and the soil. Minimum Factors of Safety against pull-out actions are taken equal to $SF=1.5$ and 2.0 for ULS and SLS conditions respectively, as advised by API RP 2A-WSD, 2000. Since extreme condition give rise to the highest mooring line tensions, anchor design is typically performed for ULS.

Code provisions make a special reference for the optimal location of the padeye, i.e. the connection point between the tensioned cable and the suction caisson. It is advised to place the padeye at a location that generates a translational mode of failure without rotation of the anchor to best exploit the capacity/stiffness reserves of the mooring system. Based on the design loads tabulated in Table 1, a Suction Caisson of diameter $D = 6$ m, embedment length $L = 6$ m ($L/D = 1$) and thickness $t = 0.024$ m (which satisfies with the $D/t = 250$ code provision) was found to best comply with the aforementioned requirements, while the padeye location lies at the edge of the caisson lid. It is interesting to note, that compared to usual caisson configurations (where the padeye is buried within the soil to maximize performance) – this configuration is definitely preferable in terms of installation and maintenance,

since the cable remains accessible over its entire length. Apparently, this is accommodated by the – deliberately chosen – large diameter caisson which provides a sufficiently large level arm for the ‘necessary’ counterclockwise moment to develop. The caissons inclined pull-out capacity and respective secant stiffness are plotted in Figure 3 below, for both ‘sealed’ and ‘unsealed’ conditions.

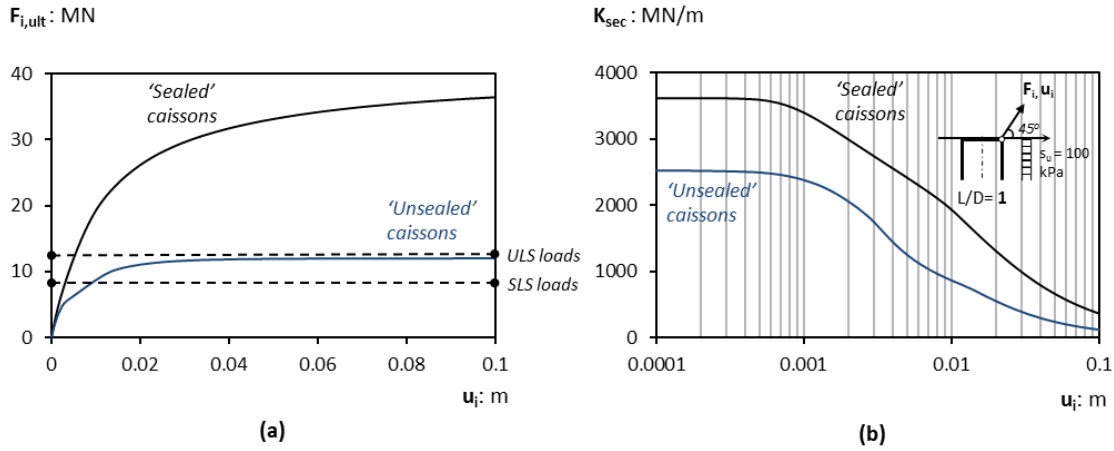


Figure 3. FEA results on (a) the inclined pull – out capacity $F_{i,ult}$ and (b) respective secant stiffness K_{sec} of the employed suction caissons, considering ‘sealed’ and ‘unsealed’ conditions.

Table 1. ULS and SLS caisson design loads.

<i>Windward Cable</i>	T_c : MN	$T_{c, design}$: MN
ULS [S.F.=1.5]	12.2	18.3
SLS [S.F.=2.0]	8.0	16.0

3. EARTHQUAKE PERFORMANCE OF THE GUYED SYSTEM

According to the 2013 European Seismic Hazard Map (SHARE, 2009 – 2013), the design ground acceleration for the chosen installation location (North-Western Adriatic Sea) is $A=0.3g$. To comply with the regional seismicity pattern, neighboring seismic events have been utilized as input motions for our study, namely:

- the 6.3 M_w L’ Aquila earthquake in the Abruzzi region of central Italy (2009) [Station: IT.ACIV, E-W component] and
- the 5.9 M_w Emilia Romagna earthquake (2012) [Station: IT.MRN, N-S component].

For the set of seismic analyses, boundary conditions of the employed numerical model are changed to realistically reproduce ground shaking conditions. Dashpot elements are introduced at the model base, to correctly simulate radiation damping, while kinematic constraints are used to between the lateral boundaries of the FE model to simulate free-field response. The loading combination assumes simultaneous action of seismic and environmental loading, with the presence of 70% of wind loading under normal operating conditions at the time that the earthquake strikes. Foundation performance is assessed on the basis of serviceability limits. To this end, following the DNV-OS-J101 deformation criteria for OWTs, it should be ensured that the accumulated (permanent) displacements at the foundation level will not introduce rotation exceeding 0.25 deg (i.e., 0.044 mrad) at the top of the supporting system (i.e., at the level of the connection point).

The resulted free-field acceleration and displacement time-histories are plotted in Figure 4, along with

their elastic response spectra corresponding to a damping ratio of $\xi=2\%$. The EC8 design spectrum at the OWT site (corresponding to stiff clay profile of Category C) is also plotted on the graphs for ease of reference. The first two eigen-periods of the OWT are denoted on the elastic spectra plots. The first eigen-mode of the flexible turbine ($T_{tower,1} = 3.12$ s) lies within a range of low spectral accelerations. The second eigen-mode, however, appearing at $T_{tower,2} = 0.56$ s, is associated with higher accelerations of the order of 1g for both records.

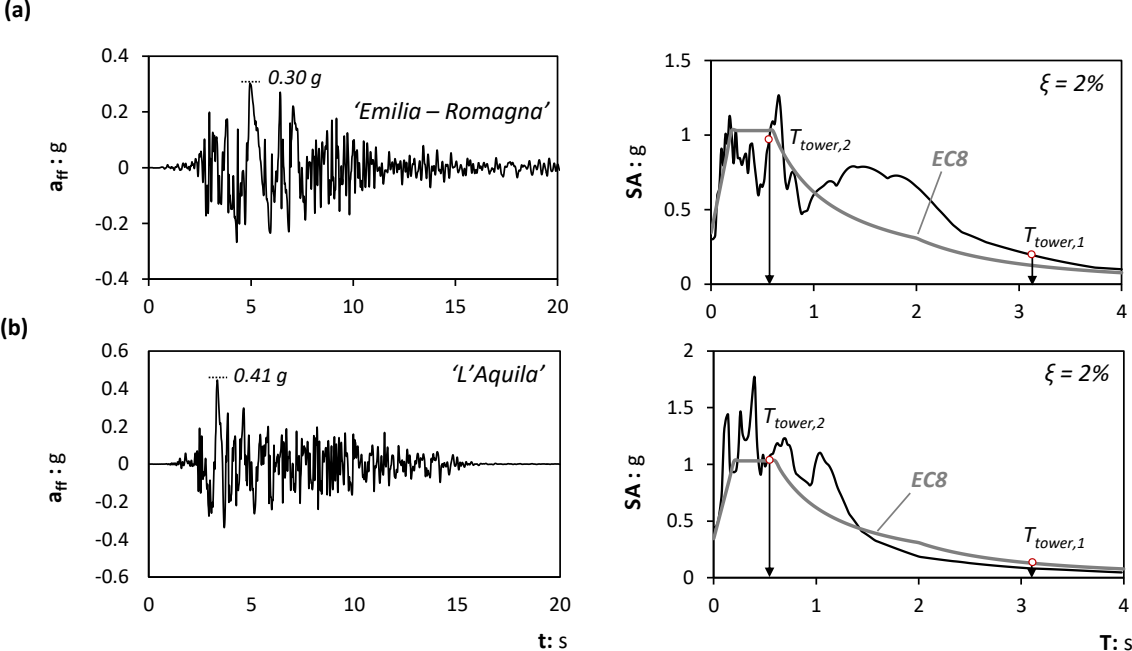


Figure 4. FEA results on the free-field response during seismic loading in terms of acceleration time-histories and respective elastic response spectra for (a) L' Aquila record and (b) Emilia Romagna record.

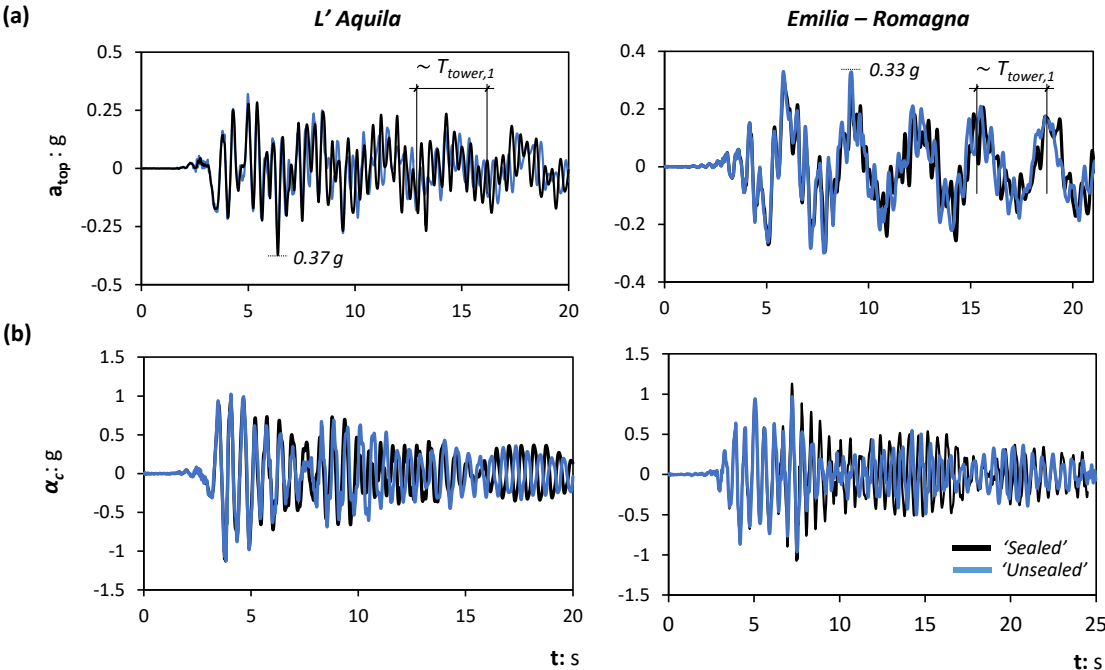


Figure 5. Tower seismic response in terms of acceleration time-histories at (a) the tower top and (b) the cables connection point (L' Aquila record on the left, Emilia Romagna record on the right).

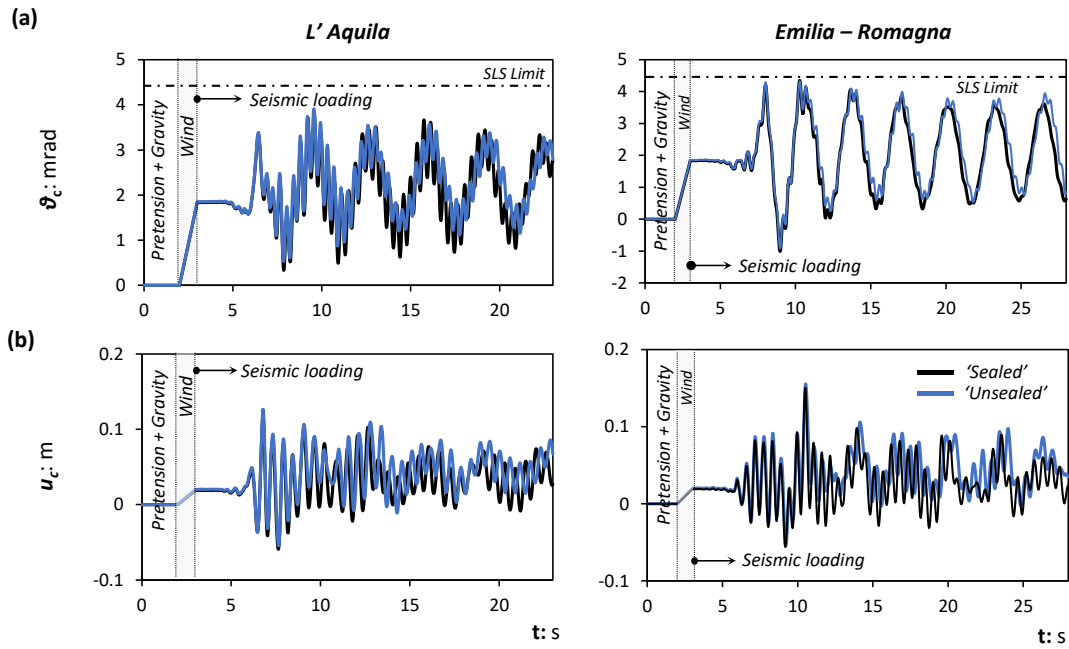


Figure 6. Results on seismic response at the cables connection point, in terms of: (a) rotation time-histories and (b) displacement time-histories (L' Aquila record on the left, Emilia Romagna record on the right).

The seismic response of the structural components of the guyed OWT tower is displayed in Figures 5-6. It is decomposed into the response of a very flexible upper sub-system (described by the oscillation of the tower top) and that of the less-compliant sub-system (described by the oscillation of the connection point). The first oscillates with the system's 1st eigen-frequency (Fig.5a), while the second displays a higher frequency oscillation dominated by the 2nd mode of vibration (Fig.5b). This coupled tower response is very well illustrated in the acceleration time histories of the tower top, where high-frequency 'wrinkles' from the sub-system's oscillation are superimposed in the more flexible response of the tower head. The assumption of a 'sealed' or 'unsealed' caisson configuration does not seem to affect the response of the turbine tower, as reflected in the rotation and horizontal displacement time-histories of the cables connection point, (plotted in Figure 6), although the 'unsealed' caissons (due to their lower stiffness) result to a slightly more flexible system with prolonged natural period. Apart from that, the dynamically attained rotation θ_c remains below the previously prescribed SLS limit for the scenarios analyzed, while there is no evidence of any permanent dislocation (if the wind load is subtracted) even in the unfavorable scenario of 'unsealed' caissons.

The seismic performance of the suction anchors is presented in detail in the plots of Fig. 7, in terms of relative horizontal and vertical displacements at the padeye location. Horizontal displacements refer to the relevant seismic displacements with respect to the movement of the ground surface, computed by subtracting the free-field motion from the actually recorded movement. Results are presented for both 'sealed' and 'unsealed' caissons. Clearly the sealed anchors (black lines) are performing in an almost quasi-elastic manner as may be witnessed from the very low-amplitude displacement values (less than 1 cm) experienced in both seismic events. On the other hand, un-sealed caissons tend to accumulate deformations throughout shaking, resulting in a permanent dislocation that heavily overtops the dislocation produced by the wind load only. For example, in the Emilia Romagna event, the ultimate horizontal displacement at the windward anchor was in the order of 30 mm, whilst only 8 mm of them are attributed to the wind load.

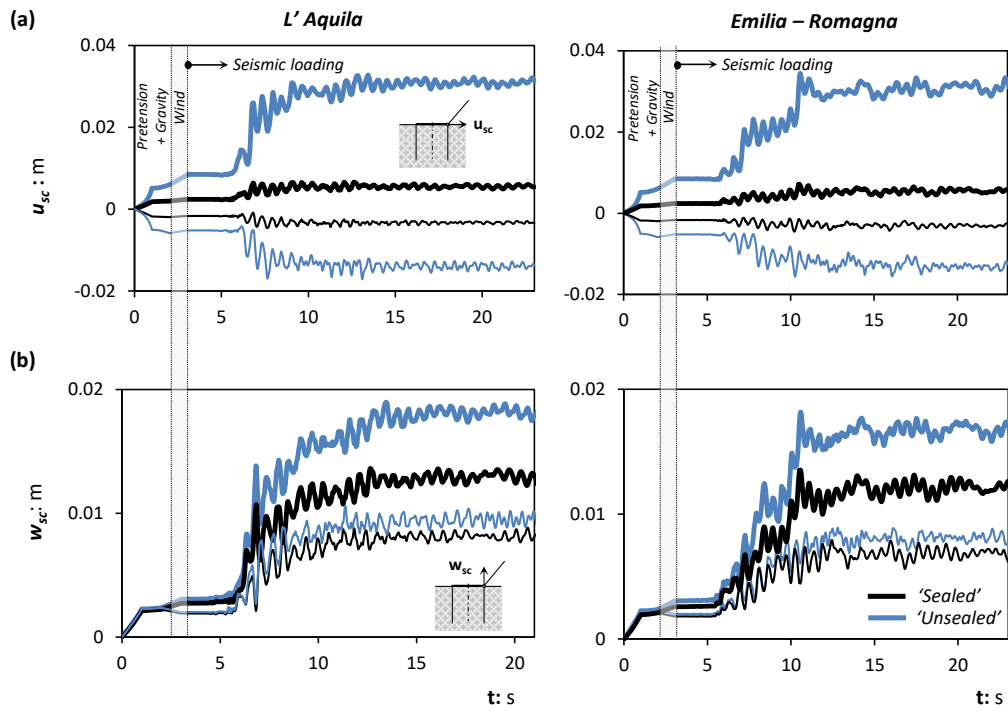


Figure 7. Foundation response to the combined wind and seismic loading scenarios, in terms of: (a) horizontal caisson displacement and (b) vertical caisson displacement. Thick lines stand for the windward caisson and thin lines for the leeward caisson. On the left: L' Aquila record; On the right: Emilia Romagna record.

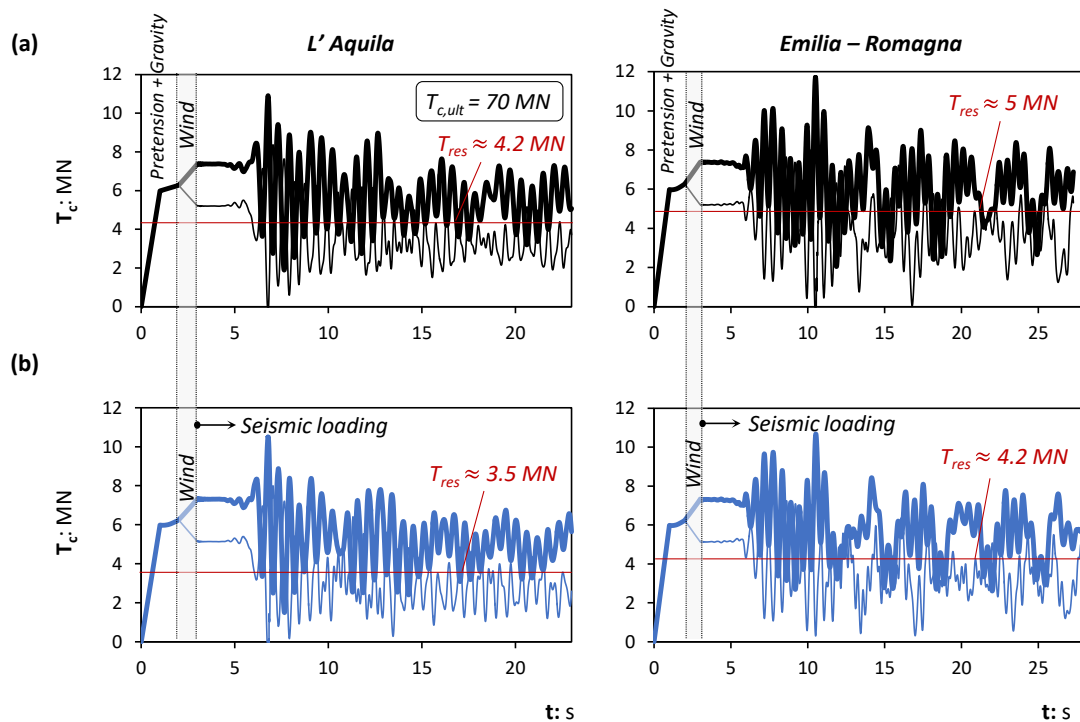


Figure 8. Cable tension time-histories for the cases of (a) 'sealed' caissons and (b) 'unsealed' caissons, during the L'Aquila (on the left) and 'Emilia Romagna' (on the right) seismic records. Thick line stands for the windward cable and thin line stands for the leeward cable response.

Cable tension time-histories around the cable top are plotted in Figure 8. It is worth mentioning, that for both events that tower experiences instances of complete slag (i.e. zeroing of pretension) at the leeward cables. However, this momentarily developed loss of support doesn't seem to endanger the system's integrity. Moreover, in all scenarios examined, the mean cable tension is gradually decreasing, reaching equilibrium at a quite lower value, compared to the one at the beginning of shaking (approximately $T_{o,w} = 7.5$ MN and $T_{o,l} = 5$ MN for the windward and leeward cables respectively). Focusing at the response of the 'sealed' caissons system, where anchor deformations are negligible and the cables may be assumed as 'fixed' on the ground, this tension loss may only be explained by observing in detail the dislocation pattern of the central footing. As vividly illustrated in the settlement-rotation curve of Figure 9, the footing is subjected to a combined shearing mechanism stemming from inertial superstructural loading and simultaneously introduced kinematic stressing generated by the propagating seismic waves (that continue to shear the foundation soil even when the inertial loading is low). As such, the footing keeps settling in every single seismic pulse resulting in a non-trivial residual settlement of about 5.5cm. The latter is interpreted as vertical dislocation at the cable-connection point, and eventually to some seismic-induced degradation in the mean value of cable pretension. Naturally, this trend is amplified further (by an approximately 0.7 MN loss in tension) when 'unsealed' caisson conditions are assumed.

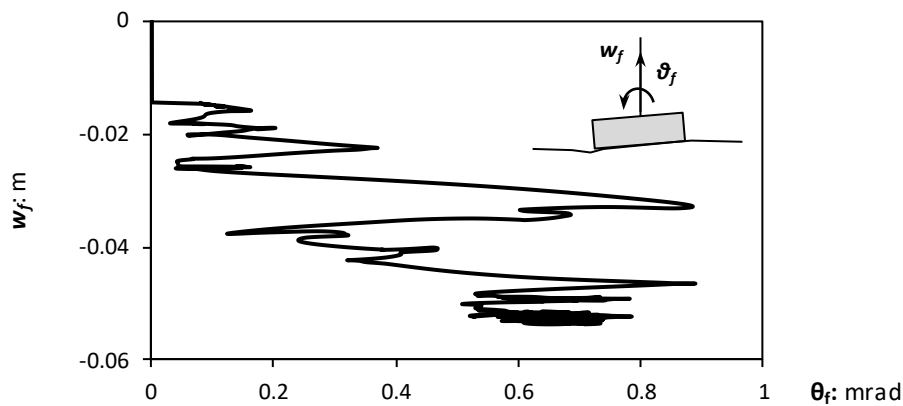


Figure 9. Settlement – rotation curve of the shallow footing during the Emilia Romagna event.

6. CONCLUSIONS

The paper investigates the performance of a cost-efficient and easy-to-install guyed foundation concept for large capacity wind turbines in intermediate water depths. The system's performance is explored numerically employing a case study, where the 10^{MW} NOWITECH reference turbine is installed in the seismically – active waters of the North-Western Adriatic Sea.

It is concluded that the system manages to undertake the seismically-induced deformations, through small displacements at the cable connection point, thus displaying an excellent behavior. The performance of the taut mooring lines is also judged as satisfactory. Although zeroing of the pretension loading occurs momentarily throughout shaking, the overall stability of the tower is not endangered. When suction is accounted for at the system's anchors, the seismically induced deformations are practically zero. Even for the highly improbable case of 'unsealed' conditions during seismic shaking, however, the developed deformations (although significantly augmented) are not large enough to have a negative impact on the tower's response. On the contrary, higher factors of safety should be proposed for the design of the central footing, to control the rate of accumulated settlements. Otherwise, the tension of the mooring lines is expected to degrade substantially during shaking, thus exposing the OWT to uncontrolled slag-instances.

7. ACKNOWLEDGEMENTS

This research study has been financially supported by the Greek State Scholarship Foundation (IKY Fellowships of Excellence for Postdoctoral Studies in Greece -MIS 5001552).

8. REFERENCES

- ABAQUS 6.13 (2013). Standard user's manual. *Dassault Systèmes Simulia Corp.*, Providence, RI, USA.
- API (2000). Recommended practice for planning, designing and constructing fixed offshore platforms—working stress design. *API recommended practice 2A-WSD (RP2A-WSD)*, 21st Ed, American Petroleum Institute, Washington DC.
- Anastasopoulos I, Gelagoti F, Kourkoulis R, Gazetas G. (2011). Simplified Constitutive Model for Simulation of Cyclic Response of Shallow Foundations: Validation against Laboratory Tests, *Journal of Geotechnical and Geoenvironmental Eng., ASCE*, 137 (12): 1154-1168.
- Bastick N. (2009). Blue H - The World's First Floating Wind Turbine. *The First Dutch Offshore Wind Energy Conference, "Essential Innovations"*, November 12 -13, 2009, Den Helder, The Netherlands. (Presentation)
- Bratland S. (2009). Hywind - The World First Full-scale Floating Wind turbine. *Seminar and B2B meetings "Powering the Future – Marine Energy Opportunities"*, November 5, 2009, Lisbon, Portugal. (Presentation)
- Bransby MF, Yun GJ. (2009). The undrained capacity of skirted strip foundations under combined loading. *Géotechnique*, 59(2), 115-125.
- Bulder BH, Van Hees MT, Henderson A, Huijsmans RHM, Pierik JTG, Snijders EJB, Wijnants GH, Wolf MJ (2002). Study to feasibility of and boundary conditions for floating offshore wind turbines. ECN, MARIN, Lagerway the Windmaster, TNO, TUD, Technical Report, (2002-CMC), R43.
- Chen SS, Chung H. (1976). Design guide for calculating hydrodynamic mass. Part I: Circular Cylindrical Structures. Components Technology Division, Argonne National Laboratory, Argonne, Illinois.
- Det Norske Veritas (2010). *Offshore Standard DNV-OS-E301, Position Mooring*. Det Norske Veritas, Høvik.
- Det Norske Veritas (2014). *Offshore Standard DNV-OS-J101, Design of Offshore Wind Turbine Structures*. Det Norske Veritas, Høvik.
- Morison JR, Johnson JW, Schaaf SA (1950). The force exerted by surface waves on piles. *Journal of Petroleum Technology*, 2(05), 149-154.
- Randolph MF, House AR (2002). Analysis of suction caisson capacity in clay. *Offshore technology conference*.
- Telecommunications Industry Association (2005). Structural standards for Steel Antenna Towers and Antenna Supporting Structures. TIA/EIA-222-G, EUA.
- Tonni L, Rocchi I, Cruciano NP, Martinez MFG, Martelli L, Calabrese L. (2016). A multidisciplinary tool for the development of a regional-scale geotechnical model: a case study in the North-Western Adriatic coastal area. *Procedia Engineering*, 158, 546-551. DOI: 10.1016/j.proeng.2016.08.487.
- Weinstein A. (2009). WindFloat: A Floating Support Structure for Offshore Wind Turbines. *Seminar and B2B meetings "Powering the Future – Marine Energy Opportunities"*, November 5, 2009, Lisbon, Portugal. (Presentation)
- World Energy Council (2016). World Energy Resources Wind Report.